

A NOVEL 3-WAY CELL SORTER USING POWER EFFICIENT ELECTROLYSIS-BASED ACTUATOR

Jasbir N. Patel, Abdul Haseeb Ma, Takaya Ueda, Bonnie Gray, Ash Parmeswaran, Bozena Kaminska
Simon-Fraser University, Burnaby, BC, Canada.

Abstract

In this paper, a novel 3-way cell sorter using a power efficient electrolysis based actuator and X-flexure joint arm is presented. The small scale 3-way cell sorter is widely used in the field of bio-separation, namely immunology and haematology. Three 3-way cell sorters are also used in drug testing and analysis to sort cells in three different directions. The proposed design offers superior performance in small scale sorting applications than the other previous techniques like charged plates, T-switch, dielectrophoresis, and Fluorescence Activated Cell Sorting (FACS). A power efficient electrolysis-based actuator using water which works efficiently with 3 to 4 V is used for low power operation. Two X-flexure joint arms with individual actuators are designed and connected with X-flexure joint springs to regain the original position. The X-flexure joint also avoids direct contact of the arm to top and bottom surfaces of the channels to prevent mechanical failure. Simulation results using ANSYS® FEM tool are presented along with the proposed design with a $50\ \mu\text{m} \times 50\ \mu\text{m}$ cross-section fluidic channel that can be customized as required. The total area occupied by the proposed design is $700\ \mu\text{m} \times 700\ \mu\text{m}$. The simulation results show efficient operation of the proposed design with 18 mm/min flow rate.

Keywords: 3-way cell sorter, Electrolysis Actuator, X-flexure joint spring, Bio-separation, Flow cytometry.

1. Introduction

Sorting and separation of cells are important for bio-separation applications. Small scale cell separation is extensively used in the study of immunology and haematology [1]. Cell sorters are widely used to sort cells in different directions in drug testing and analysis. Different methods for sorting have been previously investigated. Some of the known cell sorters are charged plates, T-switch, dielectrophoresis [2], and Fluorescence Activated Cell Sorting (FACS) [3]. Main concern for efficient cell sorters is pH and temperature variation of sample fluid due to actuators used to sort the cells. Different methods to minimize these issues in cell sorting have been proposed previously. All of the aforementioned methods have pros and cons but here only two of the most popular ones are briefly explained.

The charged plate method utilizes two plates with a large voltage difference of about 5000 V to attract and sort cells. The cells are enclosed in a droplet of carrier solution; the droplets are positively or negatively charged or uncharged according to the results obtained through flow cytometry. The charged droplets are attracted towards the opposite charged

plate to be sorted and the uncharged droplets will move unaffected between the plates, and are usually treated as waste [4]. The advantage of this method is the high throughput of 10^6 cells per hour with high accuracy. However, the throughput and accuracy decreases as the cells become large ($50\ \mu\text{m}$), because accurate droplet formation becomes more difficult. Also it requires a high voltage of 5000 V to operate [3][4].

In contrast, T-switch cell sorting is a method that mechanically sorts cells into two groups by moving a bubble actuated T-switch. Bubbles are formed by water electrolysis through platinum electrodes, pushing the T-switch which causes the channel direction to change. When a cell is intended to steer in the opposite direction, bubbles in the opposite chamber are generated to shift the T-switch to the other state [5]. This device uses a low operating voltage of 3.2 V. Even though, the frequency response of the switch is only about 3 Hz, the structure is applicable for small scale cell sorting [5]. The negative aspect of this design is the rotational design of the free falling T-switch. Free falling switch can fail if the structures in contact with bottom or top stick due to microscopic changes in the sliding area; this failure occurs before material failure involving fatigue or fracture [6]. Furthermore, to sort the cells in three or more direction requires multiple sequence of the same design which increases over-all device size and dead volume of the fluid.

In order to overcome the limitations discussed above, a novel 3-way and small scale sorter is proposed here. Furthermore, it can accommodate any size of typical biological cell. The proposed design is also designed using a non-fully released X-flexure joint to avoid failure due to stiction. The X-flexure joint spring also helps the arm to regain its original position as soon as the force from actuator is removed. The device is also intended to operate with the electrolysis-based actuator using 3-4 V supply without a noticeable change in pH and temperature of the channel fluid. Fabrication steps are also given for a silicon bulk micro-machining based process. To show proof-of-concept of the design, simulation results using ANSYS® are provided.

In Section 2, the proposed design is discussed in detail. Then, the proposed fabrication process for the proposed 3-way cell sorter is given in section 3. The results are discussed in section 4 followed by the conclusion in section 5.

2. Proposed Design

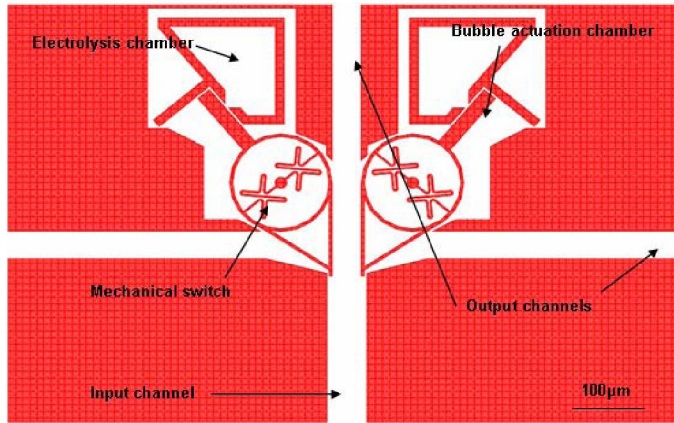


Figure 1: Proposed Design of 3-Way Cell Sorter

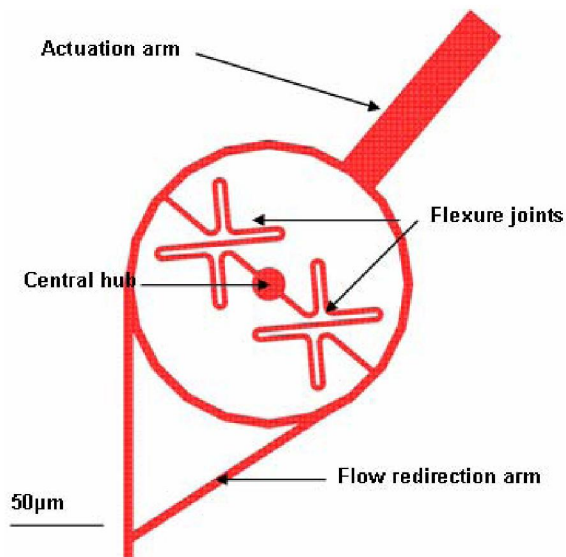


Figure 2: Mechanical Switch Design with X-Flexure Joint

The layout drawing of the 3-way cell sorter is shown in Figure 1 above. The main parts of the proposed design are two mechanical switches with X-flexure joints, electrolysis chamber, electrolysis electrodes, actuation chamber and channels. Depth of all the structures is 50 μm .

2.1. Design of X-flexure joint arm based switch

The two X-flexure joint arms are the most important components of the proposed design which are used to redirect the cell flow. The detailed drawing of the X-flexure arm is shown in Figure 2. Each arm is comprised of a central hub, a flow redirection arm, and an actuation arm. The actuation arm and the flow redirection arm are connected to the central hub by two X-flexure springs. The central hub is firmly connected with top and bottom surfaces whereas rest of the switch is separated by 2-3 μm from top and bottom. The angle of rotation of the switch is 19°.

Previous research [7] demonstrated that in-plane rotation of a flexure joint is independent of the shape of the joint, and its stiffness is dependent only on the total length of the joint. The X-shaped flexure joint is chosen to achieve large rotation. The unfolded length of the X-flexure joint is 340 μm . If the unfolded flexure joint is modeled as a simple cantilever with concentrated force applying at the free end, its mechanical stiffness can be calculated [8],

$$k = \frac{3EI}{l^3} \quad \text{Equation 1}$$

where E is the Young's modulus of the bulk silicon crystal, I is the moment of inertia, and l is the length of the cantilever beam. The joint has a rectangular cross-section, with a depth of 50 μm and width of 3 μm . Hence, the moment of inertia can be calculated as,

$$I = \frac{wd^3}{12} \quad \text{Equation 2}$$

2.2. Operation principle of the proposed design

From the flow cytometry identification of the cells, as an example assume that the cell should be sorted in the left channel. To activate the left X-flexure joint arm, a voltage potential is applied to the interdigitated positive and negative electrodes. Because of the electrolytic reaction of the water, hydrogen and oxygen gas are produced. The amount of gas produced at electrodes is governed by Faraday's Law,

$$\Delta n = \frac{3}{4F} \int_0^t I \cdot d\tau \quad \text{Equation 3}$$

where, Δn is the number of moles of gas generated, F is the Faraday's constant, I is the electrical current, and t is the time of current flow. The pressure exerted by the bubble is proportional to its surface tension σ and inversely proportional to the bubble radius r ,

$$\Delta P = \frac{2\sigma}{r} \quad \text{Equation 4}$$

The force being exerted by the gas bubble can be approximated by the mechanical relation between pressure and force,

$$F = PA = \frac{2\sigma}{r} \times A \quad \text{Equation 5}$$

where, A is the active area. Hence, maximizing the contact area and minimizing the radius of curvature would result in maximum actuation force. This force will move the X-flexure joint arm to redirect the channel fluid flow in the left channel causing the identified cell to be sorted into the left channel. As soon as the voltage applied to the electrodes is removed, the X-flexure joint will regain its original position because of the spring action of the X-flexure joint and the channel fluid will flow in the straight direction. Similarly, the right arm can also be activated by applying voltage to the electrodes on the right actuation chamber.

3. Fabrication Process

The proposed design involves fabrication of two parts: 1) the structural part with channels and X-flexure joint on a silicon substrate and 2) the glass lid with electrolysis electrodes.

3.1. Fabrication of channels and joint

Two silicon wafers are used to fabricate the channels and the joint. The fabrication steps are outlined in Figure 3.

First, the trenches (2-3 μm) are etched in the active are of the X-flexure joint arm (Figure 3(a)). A second wafer is bonded by fusion bonding and thinned to 50 μm . Similar trenches as previous step are made on top of this now 50 μm thick wafer (Figure 3(b)). Finally, the channels, chambers and joint structures are created by Deep Reactive Ion Etching (DRIE) of the 50 μm wafer (Figure 3(c)).

3.2. Fabrication of glass cover

The electrolysis electrodes of platinum are fabricated in the top glass lid. The fabrication steps for the glass lid are shown in Figure 4. First, photoresist is patterned onto the glass (Figure 4(a)). Then, titanium, as an adhesive material, and platinum, as the actual electrode material, are deposited using sputtering (Figure 4(b)). The photoresist and the unwanted metals are removed by acetone lift-off (Figure 4 (c)). Finally, the inlet and outlets are drilled using a CO₂ laser [5].

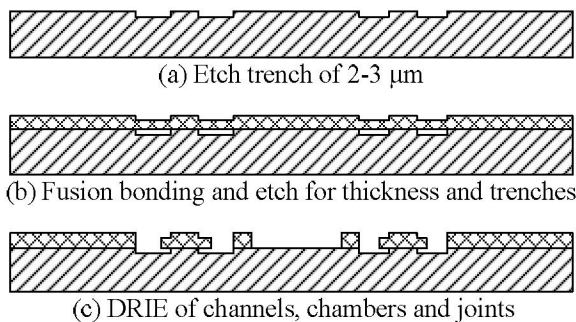


Figure 3: Proposed Fabrication Process for Channel and Joint

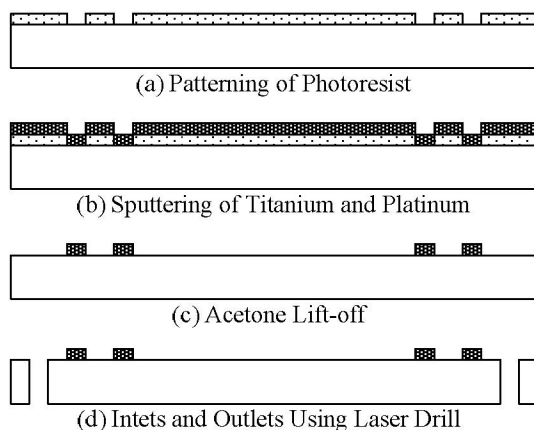


Figure 4: Proposed Fabrication Process for Glass Cover

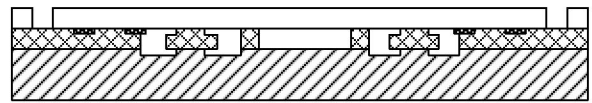


Figure 5: Final Cross-Section of the Proposed Design

3.3. Wafer bonding

The silicon wafer and the glass lid are anodically bonded using at 1000 V and 340 C to create the final structure as shown in Figure 5.

4. Simulation

The ANSYS® Multiphysics™ software was used to simulate the design. Modeling of the proposed design in ANSYS® is split into two major parts. The first simulation is done for the fluidic channel when the flow is redirected. The second simulation is done to model the mechanical behavior of the X-flexure joint.

4.1. Micro-channel simulation

These simulations are carried out to measure the pressure on the redirection arm because of input fluid velocity. Simultaneously, velocity of the fluid is also simulated to verify flow redirection. For simplicity, laminar flow of the main channel fluid is assumed with 18 mm/sec. Furthermore, back pressure at the outlet is also assumed zero.

The simulation results for the pressure and velocity are shown in the Figure 6 and Figure 7 respectively. From Figure 6, the maximum pressure is observed near the input end. The pressure at the redirection arm is predicted to be less than 3.709 Pa. Similarly, Figure 7 shows the effective redirection of the main channel fluid for the desired sorting operation. The results show that the maximum velocity of the fluid is at the output end and is expected to be 561 $\mu\text{m}/\text{sec}$ with velocity at the channel walls near zero.

4.2. Mechanical switch simulation

The goal of this simulation is to observe and predict the required force to rotate the X-flexure joint arm. In addition, the stress level in the X-flexure joint is monitored to ensure the rotational movement without mechanical failure. Simulation results measured from the fluidic channel simulation is also considered to predict the amount of pressure exerted on the flow redirection arm while the device is operating.

The material model is set with the properties of single-crystal silicon: Young's Modulus is set to 190GPa, Poisson's Ratio is set to 0.22, and density is set to 2330 kg/m^3 [9]. The model of the mechanical arm is imported from the layout designed in Cadence. The central hub is anchored down by setting the degree of freedom equal to zero in all directions. Pressure of 4.173Pa is applied to the flow redirection arm in the opposite direction of movement to model the pressure from the channel fluids.

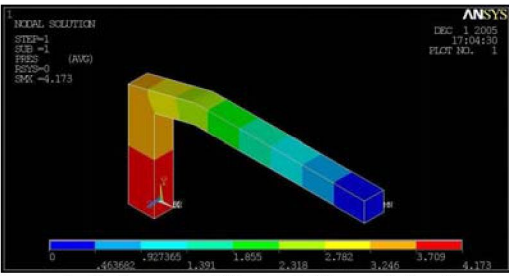


Figure 6: Orthogonal View of Channel for Pressure

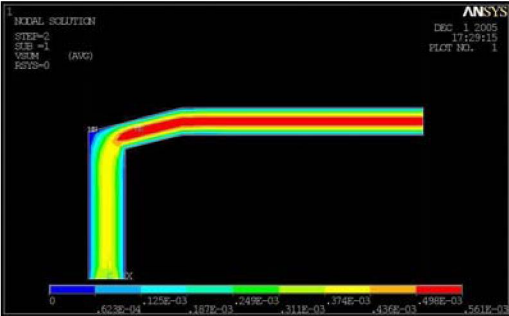


Figure 7: Cross-Sectional View of Channel for Velocity

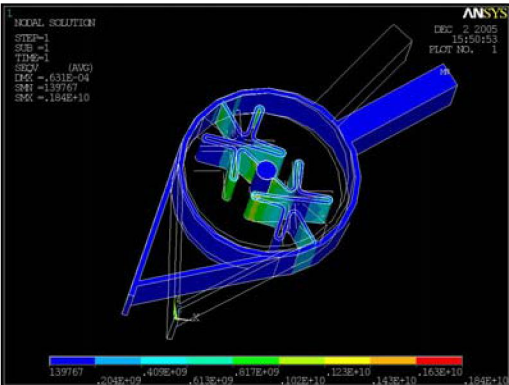


Figure 8: Stress Plot on Switch

By varying the amount of pressure exerted on the actuation arm, the amount of displacement of the mechanical switch can be observed in the simulation results. For 19° rotation of the X-flexure joint, approximately 250kPa pressure is required. Figure 8 shows a von Mises stress plot of the mechanical switch after it has rotated 19°. The maximum stress experienced by the switch is only 1.84GPa which is well below the failure stress of silicon (7GPa); Hence, the switch should be able to rotate 19° without breaking [9].

The reliability and repeatability of the electrolysis with 3 to 4 V is already proved in previous work [5]. Hence, the satisfactory operation of the proposed design should result in adequate operation. However, the operating frequency of the proposed design can only be measured after actual fabrication.

5. Conclusion

A novel 3-way cell sorter using a power efficient electrolysis based actuator and X-flexure joint arm is presented which offers superior predicted performance in small scale sorting

applications than previous techniques. A power efficient electrolysis-based actuator which works efficiently with 3 to 4 V is also used. Also presented is an X-flexure joint arm with an individual actuator and X-flexure joint spring to help regain the original position. The X-flexure joint arm also avoids direct contact of the arm to top and bottom surfaces of the channel to prevent mechanical failure. The simulation results using ANSYS® FEM tools are also obtained to predict performance. Simulation results for a 50 μm × 50 μm cross-section of fluidic channel are presented that give satisfactory results for flow redirection. The total layout area occupied by the proposed design is 700 μm × 700 μm using Cadence Design tools. The simulation results show efficient operation of the proposed design with 18 mm/min flow rate.

References

- [1] Recktenwald, D., *Cell separation methods and applications*. Published by CRC, M. Dekker, New York, ISBN 0824798643, 1998.
- [2] Ahuja, S., *Handbook of bioseparations*. CA: Academic Press, San Diego, 2000.
- [3] Orfao, A., "General Concepts about Cell Sorting Techniques", *Clinical Biochemistry*, vol. 29(1): pp 5-9, 1996.
- [4] Ormerod, M.G., *Flow cytometry*. Oxford: BIOS Scientific, 1999.
- [5] Chen-Ta Ho, R.-Z.L., Hwan-You Chang and Cheng-Hsien Liu, "Micromachined electrochemical T-switches for cell sorting applications," *Lab on a chip*, vol. 5(11), pp. 1248-1258, 2005.
- [6] S. L. Miller, G.L., M.S. Rodgers, J.J. Sniegowski, J.P. Waters and P.J. McWhorter, "Routes to failure in rotating MEMS devices experiencing sliding friction," *Proc. of SPIE Micromachined Devices and Components III*, vol. 3224, pp. 24-30, 1997.
- [7] Heiko Fettig, J., Ted Hubbard and Marek Kujath, "Simulation, dynamic testing and design of micromachined flexible joints", *Journal of Micromechanics and Microengineering*, vol. 11: p. 209-216, 2001.
- [8] Judy, J.W., *Batch-Fabricated Ferromagnetic Microactuators with Silicon Flexures*, University of California: Berkeley, 1996.
- [9] Petersen, K.E., "Silicon as Mechanical Material", *Proceeding of the IEEE*, vol. 70, issue 5: p. 420-457, 1982.